Observation of ultrabroadband, beamlike parametric downconversion

Kevin A. O'Donnell and Alfred B. U'Ren

División de Física Aplicada, Centro de Investigación Científica y de Educación Superior de Ensenada, A.P. 360, Ensenada, Baja California, 22800 México

Received November 16, 2006; revised December 25, 2006; accepted January 5, 2007; posted January 8, 2007 (Doc. ID 77081); published March 5, 2007

We report spontaneous parametric downconversion having an unusually wide spectral bandwidth. A collinear type 1 phase-matching configuration is employed with degeneracy near the zero group-velocity dispersion frequency. With a spectral width of 1080 nm and degenerate wavelength of 1885 nm, the source also emits a high flux of $3.4\times10^{11}\ \mathrm{s^{-1}\,W^{-1}}$ photon pairs constrained to a cone of only $\approx2°$ half-angle. A rigorous theoretical approach is developed that confirms the experimental observations. The source properties are consistent with an ultrashort photon-pair correlation time and, for a narrowband pump, extremely high-dimensional spectral entanglement.

OCIS codes: 190.2620, 190.4410.

The process of spontaneous parametric downconversion (SPDC), in which pump photons split into pairs of signal and idler photons, can exhibit a wide range of emission characteristics. In particular, the spectral properties vary widely in practice and are intimately tied to the phase-matching configuration in the second-order nonlinear crystal employed. Our purpose in this Letter is to demonstrate that, when certain conditions related to phase matching are met, even a narrowband pump can produce downconversion with an exceptionally large bandwidth. These same conditions also lead to a high flux of downconverted photons emitted into a narrow, beamlike angular distribution.

The significance of broadband downconversion has been discussed previously. A large bandwidth is consistent with a short correlation time between the signal and idler photons of a given pair.[1] This time represents the resolution limit in metrology applications, such as quantum optical coherence tomography,[2] that rely on signal–idler arrival time differences. Also, for a narrowband pump, a wide downconversion bandwidth creates a two-photon state having many Schmidt mode pairs or, equivalently, high-dimensional spectral entanglement.[3] Many modes imply a large amount of mutual information, which is a measure of the information that can, in principle, be shared by two parties through spectral photon pair correlations.[4] Further, Schmidt modes can be occupied independently, so that having many available modes means that individual photon pair behavior can be preserved at high light levels. Such behavior has been demonstrated with a two-photon process that is linear instead of quadratic in its power dependence.[5]

There have been previous experimental demonstrations of broadband SPDC, where bandwidths of tens of nanometers are not uncommon. For example, in Ref. 5 a bandwidth (defined throughout as full width at half-maximum) of 31 nm was reported for periodically poled bulk KTP, while Ref. 6 obtained a bandwidth of $\approx$40 nm with a KTP waveguide, with both results being in the near infrared. Elsewhere, a downconversion bandwidth of $\approx$115 nm was reported near a mean wavelength of 840 nm.[7] In that study the frequency spread of a broadband pump was mapped into a yet wider range of downconverted frequencies. A different approach was taken in Ref. 8, which reported a bandwidth of 185 nm at a center wavelength 812 nm. In this case the pump light was narrowband but tightly focused; the bandwidth arose from phase matching the wide angular range of pump wave vectors.

In contrast, here we develop a broadband SPDC source with a narrowband, weakly focused pump. In a periodically poled crystal, energy conservation and perfect phase matching imply that[9]

$$\omega_p - \omega_s - \omega_i = 0, \tag{1}$$

$$\Delta\mathbf{k} \equiv \mathbf{k}_p(\omega_p) - \mathbf{k}_s(\omega_s) - \mathbf{k}_i(\omega_i) - \mathbf{k}_g = 0, \tag{2}$$

where the subscripts p, s, and i denote quantities associated with, respectively, pump, signal, and idler photons. Here, $\Delta\mathbf{k}$ is the wave vector mismatch, ω_j $(j=p,s,i)$ is the frequency, $\mathbf{k}_j(\omega_j)$ is the wave vector within the crystal, and $\mathbf{k}_g$ is the poling wave vector.

To produce wideband phase matching, consider the case when all vectors of Eq. (2) are collinear and are replaced by corresponding scalars. We assume a monochromatic pump with fixed ω_p but allow ω_s and ω_i to vary from the degenerate frequency $\omega_d \equiv \omega_p/2$ as $\omega_s = \omega_d + \delta\omega_s$ and $\omega_i = \omega_d + \delta\omega_i$. Expanding Δk into a power series in $\delta\omega_s$ and $\delta\omega_i$, it follows that

$$\Delta k = \sum_{n=1}^{\infty} [(-1)^{n+1} k_i^{(n)}(\omega_d) - k_s^{(n)}(\omega_d)] \delta\omega_s{}^n/n!, \tag{3}$$

where the superscripts (n) denote nth frequency derivatives, k_g has been chosen to provide perfect phase matching at degeneracy, and it has been noted that Eq. (1) implies that $\delta\omega_i = -\delta\omega_s$. In what follows, we broaden the bandwidth over which $|\Delta k|$ is small by removing terms of Eq. (3) of increasing order in $\delta\omega_s$.

0146-9592/07/070817-3/$15.00

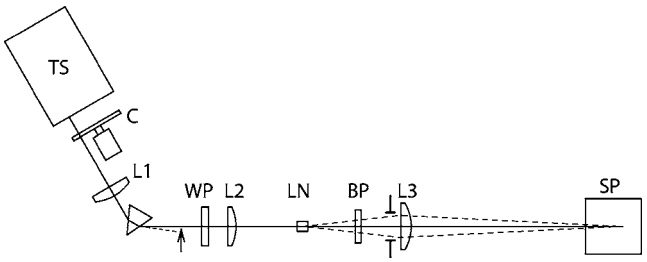

Fig. 1. Broadband downconversion experiment. The Ti:sapphire laser (TS) beam is chopped (C) and focused into a lithium niobate crystal LN by lenses L1 and L2. A half-wave plate WP rotates the pump polarization. A Si Brewster plate (BP, with plate normal directed out of figure plane) isolates the downconversion, and the emission half-angle subtended by the limiting aperture after BP defines $\Delta\theta$. The CaF_2 lens L3 focuses the light into the spectrometer SP.

First, for a type 1 interaction, $k_s(\omega_s)$ and $k_i(\omega_i)$ are associated with the same crystal index, so all terms having odd n in Eq. (3) vanish. Then, the $n=2$ term of Eq. (3) may be eliminated by choosing ω_d so that $k_{s,i}^{(2)}(\omega_d)=0$ for the particular crystal, which is the condition of zero group-velocity dispersion. The series does not then begin until the fourth order in $\delta\omega_s$, implying a wide emitting bandwidth. It is notable that these conditions can occur only at degeneracy; otherwise, the nth term of Eq. (3) contains $k_s^{(n)}$ and $k_i^{(n)}$ evaluated at different frequencies, and term cancellations for $n=1,2,3$ are not possible.

We employ periodically poled lithium niobate, with pump, signal, and idler waves polarized along the z axis and propagation along the x axis of the crystal. Using a Sellmeier equation for the extraordinary refractive index,[10] it is straightforward to calculate the temperature-dependent ω_d for which $k_{s,i}^{(2)}(\omega_d)=0$. At 20°C, this condition corresponds to a pump wavelength $\hat{\lambda}_p=2\pi c/\omega_p=958.7$ nm, which in turn implies a poling period $\hat{\Lambda}_g=2\pi/k_g=28.1$ μm from Eq. (2) at degeneracy. Thus, cancellation of all terms of Eq. (3) for $n<4$ is consistent with reasonable experimental parameters.

In experiments, the pump was a narrowband, continuous-wave, Ti:sapphire laser having ≈1 W of power[11] with a birefringent filter added to tune over 910–980 nm. As indicated in Fig. 1, lenses focused the output beam to a wide 110 μm waist inside the $L=1$ cm long crystal, which had poling periods Λ_g in steps between 25.5 and 28.7 μm at eight positions along its entrance face. The light exiting the crystal was incident on a Si Brewster plate that absorbed the pump but transmitted the downconverted flux. This flux then passed through a limiting aperture and was focused by a CaF_2 lens into a spectrometer, which employed a highly efficient Littrow grating and a sensitive cooled InSb detector. The detector signal was processed by a lock-in amplifier.

It was verified that, if either the pump or detected polarization was rotated by 90°, the detector signal fell to low levels as expected. Even at room temperature, there was no evidence of photorefractive crystal damage. It was also found that temperature tuning the crystal could flood the spectrometer with blackbody radiation but only weakly affected the SPDC spectrum, as is consistent with broadband phase matching. Thus the crystal was instead operated at room temperature, and the spectrum was width optimized by varying λ_p and Λ_g. Indeed, λ_p and Λ_g as quoted in the experimental results differ slightly from $\hat{\lambda}_p$ and $\hat{\Lambda}_g$ calculated earlier. These differences may be attributed to optimization of phase matching throughout the limiting aperture of Fig. 1.

With $\lambda_p=942.5$ nm and $\Lambda_g=27.4$ μm, Fig. 2(a) shows measured spectra for several values of the limiting aperture angular radius $\Delta\theta$. For small $\Delta\theta$, the spectrum rapidly rises with increasing $\Delta\theta$, while the curves for $\Delta\theta=1.5°$, 2.0°, 2.5° are of similar height. Most significantly, the spectra are remarkably broad. For the three larger $\Delta\theta$ of Fig. 2(a) the frequency bandwidth is $0.53\bar{\omega}$, where $\bar{\omega}$ is the average frequency; in terms of wavelength, this corresponds to an unprecedented 1080 nm bandwidth. The spectra are normalized in units of photon rate per unit frequency per watt of pump power. Integration of the spectrum for $\Delta\theta=2.5°$ implies a photon pair rate of 3.4×10^{11} $s^{-1}W^{-1}$, or a SPDC power of 3.6×10^{-8} times the incident power. These values (and, for that matter, the spectra) are internal quantities within the nonlinear crystal, which are inferred by applying calculated losses to external measurements.

In other data, we have found that for shorter λ_p the SPDC power falls; for $\lambda_p\leqslant939$ nm the spectra fall to ≤10% of the levels of Fig. 2(a). For $\lambda_p>942.5$ nm there is still significant SPDC power, but the spectra sag for frequencies near the center of Fig. 2(a). Thus, while results for other λ_p are not shown here, the results of Fig. 2(a) with $\lambda_p=942.5$ nm may be considered near optimal.

To calculate the SPDC photon number spectrum $R_1(\omega_s)$, we develop a theoretical approach based on Ref. 12. It follows that

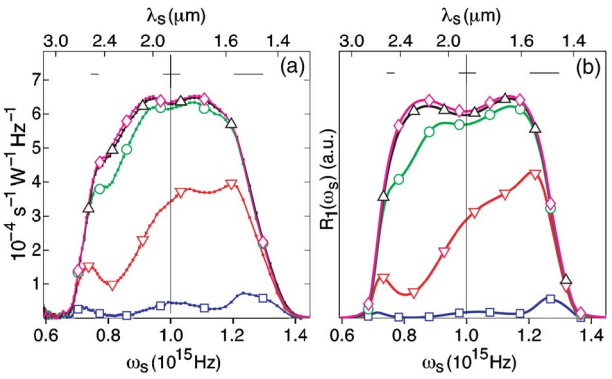

Fig. 2. (Color online) (a) Experimental downconversion spectra for a 1 cm lithium niobate crystal with poling period 27.4 μm, pumped at wavelength 942.5 nm. Cases show collection angle $\Delta\theta=0.5°$ (squares), $\Delta\theta=1.0°$ (inverted triangles), $\Delta\theta=1.5°$ (circles), $\Delta\theta=2.0°$ (triangles), $\Delta\theta=2.5°$ (diamonds). (b) Corresponding theoretical spectra for 942.5 nm, convolved over the spectrometer slit integration width. Horizontal lines denote these ω_s-dependent widths; vertical lines denote the degenerate frequency.

$$R_1(\omega_s) = \frac{\epsilon_0}{2\delta t \hbar \omega_s} \int \mathrm{d}x' \int \mathrm{d}y' \int_{z_0 - c\delta t}^{z_0} \mathrm{d}z' \left\langle \hat{I}\left(\mathbf{r}', \frac{z_0}{c}\right)\right\rangle, \tag{4}$$

where $\hat{I}(\mathbf{r},t) \equiv \hat{E}^{(-)}(\mathbf{r},t)\hat{E}^{(+)}(\mathbf{r},t)$ is the intensity operator, $\langle\cdot\rangle$ indicates an expectation value with respect to the two-photon state, z_0 is the distance along the propagation axis from the crystal to the detector, $\mathbf{r}'$ refers to coordinates outside the crystal, and $c\,\delta t$ is the length of the volume detected in time δt. In the following $\theta_{s,i}$ and $\phi_{s,i}$ denote, respectively, the polar and azimuthal internal propagation angles of the signal and idler waves. For a Gaussian pump beam with waist w_0 at the crystal midpoint, $R_1(\omega_s)$ may be written as

$$\begin{aligned} R_1(\omega_s) \propto \frac{\omega_s k_s^2 k_s^{(1)}}{n_s^2} \int_0^{\pi} \mathrm{d}\theta_s \sin\theta_s \int_0^{2\pi} \mathrm{d}\phi_s \int \mathrm{d}^3 k_i (\omega_i / n_i^2) \\ \times \eta_r(\theta_s, \phi_s) |g(\omega_s, \theta_s, \phi_s; \omega_i, \theta_i, \phi_i)|^2 \\ \times \delta(\omega_p - \omega_s - \omega_i), \end{aligned} \tag{5}$$

where the $\omega_{s,i}$ dependence of $k_{s,i}$ is now implicit, $d^3k_i = k_i^2 k_i^{(1)} \sin\theta_i \mathrm{d}\omega_i \mathrm{d}\theta_i \mathrm{d}\phi_i$, and $\eta_r(\theta_s, \phi_s)$ is of unit height only within the limiting aperture [the physical aperture function $\eta(\theta_s, \phi_s)$ is mapped to the internal $\eta_r(\theta_s, \phi_s)$ by refraction at the crystal exit face]. The function g represents the joint amplitude[13]

$$g(\omega_s, \theta_s, \phi_s; \omega_i, \theta_i, \phi_i) = \exp[-(k_\perp w_0/2)^2] \frac{\sin(\beta L)}{(\beta L)}, \tag{6}$$

where $\beta = k_\perp^2/(4k_p) - \Delta k/2$, and $k_\perp$ and Δk now follow from

$$\begin{aligned} k_\perp^2 &= k_s^2 \sin^2\theta_s + k_i^2 \sin^2\theta_i \\ &\quad + 2k_s k_i \sin\theta_s \sin\theta_i \cos(\phi_s - \phi_i), \end{aligned}$$

$$\Delta k = k_p - k_s \cos\theta_s - k_i \cos\theta_i - k_g. \tag{7}$$

In numerical integration of Eq. (5) we ignore the $(\theta_{s,i}, \phi_{s,i})$ dependence of $k_{s,i}$ itself, which is a good approximation for propagation near the pump direction. The theoretical spectra are shown in Fig. 2(b) and, with parameters as in the experiments, the agreement with Fig. 2(a) is excellent. Theoretical spectra for $\Delta\theta > 2.5°$ are not shown, but are nearly identical to those for $\Delta\theta = 2.0°$ and 2.5°; thus essentially all flux is restricted to a cone of $\approx 2°$ half-angle. This compact, beamlike angular emission is a novel property that, in future work, could be essential in obtaining high free-space or fiber-coupled collection efficiencies. There is also near symmetry about the degenerate frequency in Fig. 2(b) for $\Delta\theta = 2.0°$ and $\Delta\theta = 2.5°$. For a monochromatic pump, this symmetry is a consequence of photon energy conservation if all emitted flux is collected. For the most part, the symmetry is present in the analogous data of Fig. 2(a), although there is a slight decrease at $\omega_s \approx 0.8 \times 10^{15}$ Hz that could arise from light falling outside the collection aperture. We note that related calculations not presented here predict the signal–idler correlation time to be only 4.9 fs on the optic axis for our experimental parameters ($\lambda_p = 942.5$ nm and $\Lambda_g = 27.4$ μm).

In conclusion, we have produced downconverted light having an unprecedented bandwidth of 1080 nm at a central wavelength of 1885 nm. The wideband phase-matching conditions occur for a type 1 process with collinear downconversion at the degenerate frequency ω_d when $k_{s,i}^{(2)}(\omega_d) \approx 0$. A large flux of photons (3.4×10^{11} pairs $\mathrm{s}^{-1}\,\mathrm{W}^{-1}$) is associated with this large bandwidth, and the angle dependence of the phase mismatch restricts the light to an easily collected cone of half-angle $\approx 2°$. The experimental data presented exhibit excellent agreement in direct comparison with theoretical photon number spectra. Even though our broadband conditions occur only at a particular pump frequency ω_p for a given crystal, in principle it is possible to employ metamaterials having dispersion designed to produce such effects at any ω_p desired. The generation of photon pair states having ultrashort correlation time and an exceptionally high-dimensional spectral entanglement may, in the future, be of key importance for many applications.

We are grateful for discussions with R. S. Cudney, H. F. Alonso, S. Günther, and A. Hemmerich. This work was supported by Conacyt grants 46370-F and 49570-F. K. O'Donnell's e-mail address is odonnell@cicese.mx.

References

1. D. Strekalov, A. B. Matsko, A. Savchenkov, and L. Maleki, J. Mod. Opt. **52**, 2233 (2005).
2. M. B. Nasr, B. E. A. Saleh, A. V. Sergienko, and M. C. Teich, Phys. Rev. Lett. **91**, 083601 (2003).
3. L. Zhang, A. B. U'Ren, R. Erdmann, K. A. O'Donnell, C. Silberhorn, K. Banaszek, and I. A. Walmsley, "Generation of highly entangled photon pairs for continuous variable Bell inequality violation," J. Mod. Opt. (to be published).
4. L. Zhang, E. Mukamel, I. A. Walmsley, C. Silberhorn, A. B. U'Ren, and K. Banaszek, in *Quantum Information with Continuous Variables of Atoms and Light*, N. Cerf, G. Leuchs, and E. Polzik, eds. (Imperial College Press, 2007).
5. B. Dayan, A. Pe'er, A. A. Friesem, and Y. Silberberg, Phys. Rev. Lett. **94**, 043602 (2005).
6. A. B. U'Ren, C. Silberhorn, K. Banaszek, and I. A. Walmsley, Phys. Rev. Lett. **93**, 093601 (2004).
7. M. B. Nasr, G. Di Giuseppe, B. E. A. Saleh, A. V. Sergienko, and M. C. Teich, Opt. Commun. **246**, 521 (2005).
8. S. Carrasco, M. B. Nasr, A. V. Sergienko, B. E. A. Saleh, M. C. Teich, J. P. Torres, and L. Torner, Opt. Lett. **31**, 253 (2006).
9. L. E. Myers, R. C. Eckardt, M. M. Fejer, and R. L. Byer, Opt. Lett. **21**, 591 (1996).
10. D. H. Jundt, Opt. Lett. **22**, 1553 (1997).
11. C. Zimmermann, V. Vuletic, A. Hemmerich, L. Ricci, and T. W. Hänsch, Opt. Lett. **20**, 297 (1995).
12. Z. Y. Ou, L. Wang, and L. Mandel, Phys. Rev. A **40**, 1428 (1989).
13. A. B. U'Ren, K. Banaszek, and I. A. Walmsley, Quantum Inf. Comput. **3**, 480 (2003).